A Parametric Study of Ionian Thermal Parameters

A.C. Walker, D. B. Goldstein, P. L. Varghese, L. M. Trafton, C. H. Moore
The University of Texas at Austin; E-mail: *andrew.walker@mail.utexas.edu*

Introduction: The pre-dominant mechanism for supporting the Ionian atmosphere is still a subject of contention due to conflicting observations regarding the relative contributions of the volcanic and sublimation componens; however, nearly all observations agree that there is a signficant dayside SO_2 sublimation atmosphere. The sublimation atmosphere is highly sensitive to the SO_2 surface frost temperature; therefore, the surface frost temperature is a key variable in determining the atmospheric structure. Many groups have attempted to constrain the thermal parameters on the surface (Sinton and Kaminski, 1988; Veeder et al., 1994; Kerton et al., 1996; Rathbun et al., 2004). Here we constrain the thermal parameters based on recent observations of the column density (Jessup et al., 2004) and brightness temperature (Rathbun et al., 2004).

Model and Parametric Study: Three-dimensional Direct Simulation Monte Carlo (DSMC) simulations of Io's atmosphere are able to accurately model the rarefied flow present over much of Io (especially on the nightside). DSMC uses a representative number of molecules to statistically approximate the collisions and movements of real molecules in the gas (Bird et al., 1994). These DSMC simulations are computed in parallel on 360 processors but still require over 24 hours to complete; however, despite the complex physics included the simulations produce vertical column densities within 20% of those predicted by local vapor pressure equilibrium (LVPE) on the majority of the dayside.

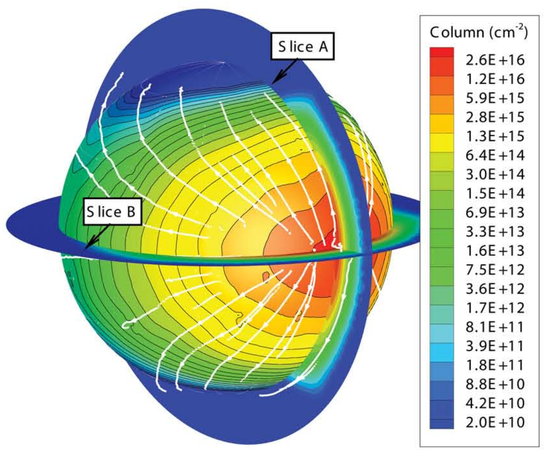

Figure 1: A DSMC simulated atmosphere showing color contours of column density. Slices A and B (with contours of number density) show the geometries along which Figures 2a and 2b were extracted. Note that the vertical scale of the slices is exaggerated by 16x.

Therefore, more rapid simulations of the surface temperature distribution will produce quite similar column densities and allow parametric study of the thermal parameters on Io's surface.

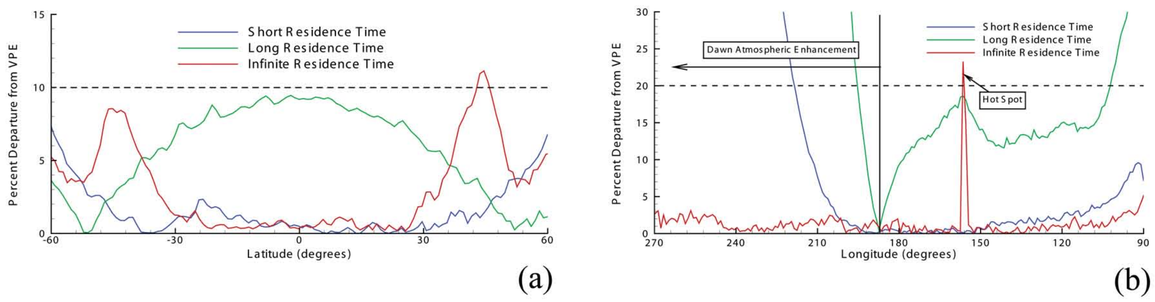

Figure 2ab: The departure from LVPE for three DSMC simulated atmospheres: i) Short residence time (Sandford and Allamandola, 1994), ii) long residence time (Walker et al., 2010), and iii) infinite residence time. The long residence time models increases the residence time by 10^3 to account for the possible high porosity of the surface. Figure 2a shows the VPE departure as a function of latitude while Figure 2b is as a function of longitude.

- Simulations match LVPE within 60° latitude of equator at subsolar longitude

- Dayside vertical column densities along equator depart further from LVPE on the morning side due to a phenomenon termed the "dawn atmospheric enhancement"

- After noon, column densities largely remain within 20% of LVPE

Thermal model: The one-dimensional heat conduction equation (1) is solved with depth for 18 x 36 points in latitude and longitude. The boundary conditions at the lower (x=D) and upper (x=0) surfaces are given by (2) and (3), respectively (Spencer et al., 1988). Q_T represents endogenic heating. Frost and non-frost surfaces are treated identically beside the differing thermal parameters.

$$\rho c \frac{\partial T(\theta,\phi,x,t)}{\partial t} = \frac{\partial}{\partial x}\left[k \frac{\partial T(\theta,\phi,x,t)}{\partial x} \right] \quad (1)$$

$$k \frac{\partial T(\theta,\phi,x,t)}{\partial t}\bigg|_{x=D} = Q_T \quad (2)$$

$$k \frac{\partial T(\theta,\phi,x,t)}{\partial x}\bigg|_{x=0} = \varepsilon\sigma T^4(\theta,\phi,x=0,t) - (1-\alpha)\left(F_S(\theta,\phi,t) + F_J(\theta,\phi)\right) \quad (3)$$

Parametric Study Summary

1. Invert column density data (Jessup et al., 2004) assuming LVPE to find inferred T_{FROST}

2. Parametrically vary frost thermal parameters in heat conduction code

3. Compute surface frost temperature distribution

4. Compare computed and inferred T_{FROST} and calculate best fit based on least squares error method

5. Assume fixed frost thermal parameters (the best fit parameters derived from [4]) when parametrically varying non-frost thermal parameters

6. Compute surface brightness temperature distribution

7. Compare computed and observed T_{BRIGHT} and calculate best fit based on least squares error

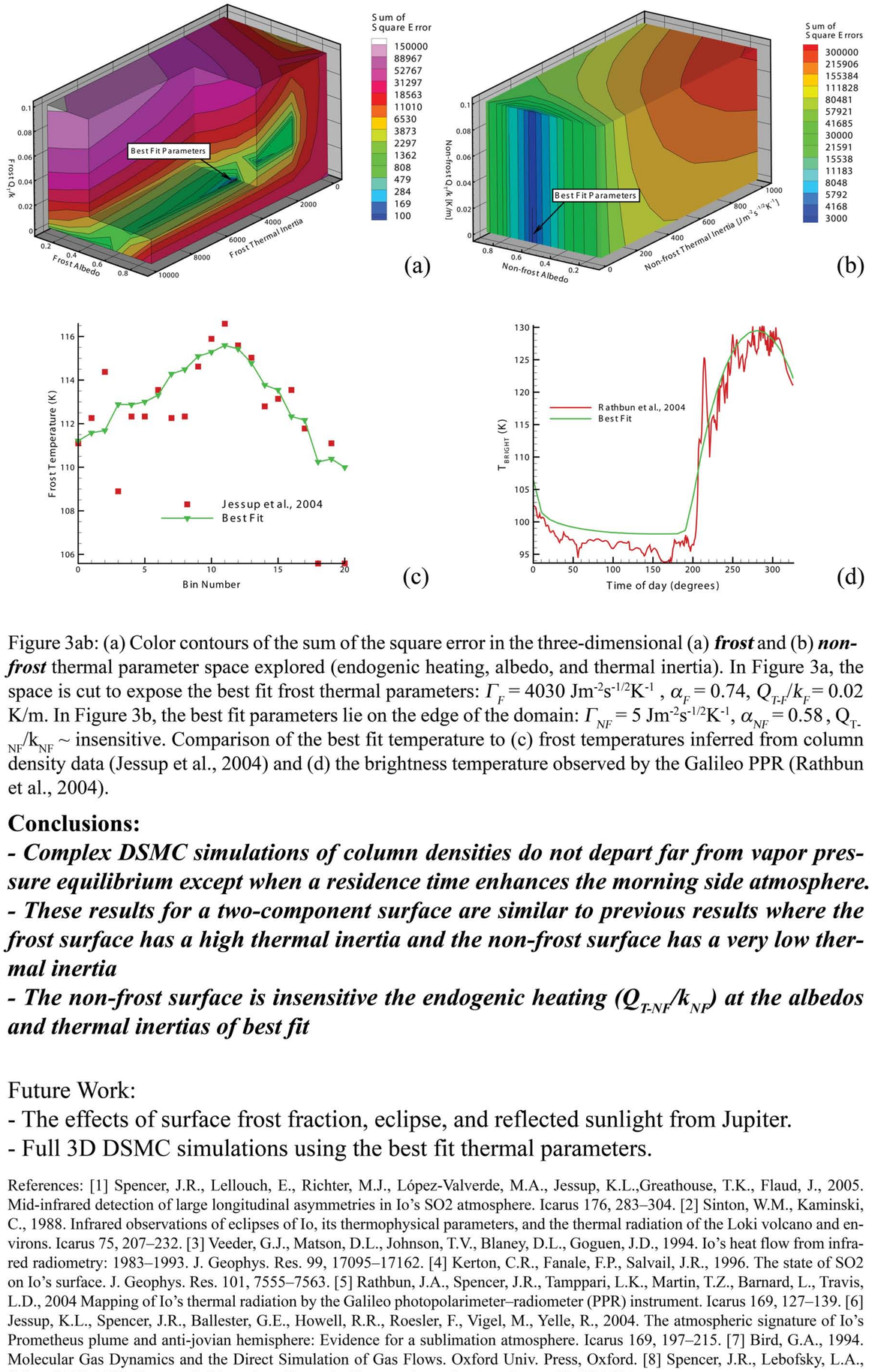

Figure 3ab: (a) Color contours of the sum of the square error in the three-dimensional (a) ***frost*** and (b) ***non-frost*** thermal parameter space explored (endogenic heating, albedo, and thermal inertia). In Figure 3a, the space is cut to expose the best fit frost thermal parameters: $\Gamma_F = 4030$ Jm^{-2}s$^{-1/2}$K^{-1} , $\alpha_F = 0.74$, $Q_{T\text{-}F}/k_F = 0.02$ K/m. In Figure 3b, the best fit parameters lie on the edge of the domain: $\Gamma_{NF} = 5$ Jm^{-2}s$^{-1/2}$K^{-1}, $\alpha_{NF} = 0.58$, $Q_{T\text{-}NF}/k_{NF}$ ~ insensitive. Comparison of the best fit temperature to (c) frost temperatures inferred from column density data (Jessup et al., 2004) and (d) the brightness temperature observed by the Galileo PPR (Rathbun et al., 2004).

Conclusions:

- Complex DSMC simulations of column densities do not depart far from vapor pressure equilibrium except when a residence time enhances the morning side atmosphere.
- These results for a two-component surface are similar to previous results where the frost surface has a high thermal inertia and the non-frost surface has a very low thermal inertia
- The non-frost surface is insensitive the endogenic heating ($Q_{T\text{-}NF}/k_{NF}$) at the albedos and thermal inertias of best fit

Future Work:
- The effects of surface frost fraction, eclipse, and reflected sunlight from Jupiter.
- Full 3D DSMC simulations using the best fit thermal parameters.

References: [1] Spencer, J.R., Lellouch, E., Richter, M.J., López-Valverde, M.A., Jessup, K.L.,Greathouse, T.K., Flaud, J., 2005. Mid-infrared detection of large longitudinal asymmetries in Io's SO2 atmosphere. Icarus 176, 283–304. [2] Sinton, W.M., Kaminski, C., 1988. Infrared observations of eclipses of Io, its thermophysical parameters, and the thermal radiation of the Loki volcano and environs. Icarus 75, 207–232. [3] Veeder, G.J., Matson, D.L., Johnson, T.V., Blaney, D.L., Goguen, J.D., 1994. Io's heat flow from infrared radiometry: 1983–1993. J. Geophys. Res. 99, 17095–17162. [4] Kerton, C.R., Fanale, F.P., Salvail, J.R., 1996. The state of SO2 on Io's surface. J. Geophys. Res. 101, 7555–7563. [5] Rathbun, J.A., Spencer, J.R., Tamppari, L.K., Martin, T.Z., Barnard, L., Travis, L.D., 2004 Mapping of Io's thermal radiation by the Galileo photopolarimeter–radiometer (PPR) instrument. Icarus 169, 127–139. [6] Jessup, K.L., Spencer, J.R., Ballester, G.E., Howell, R.R., Roesler, F., Vigel, M., Yelle, R., 2004. The atmospheric signature of Io's Prometheus plume and anti-jovian hemisphere: Evidence for a sublimation atmosphere. Icarus 169, 197–215. [7] Bird, G.A., 1994. Molecular Gas Dynamics and the Direct Simulation of Gas Flows. Oxford Univ. Press, Oxford. [8] Spencer, J.R., Lebofsky, L.A., Sykes, M.V., 1988. Systematic biases in radiometric diameter determinations. Icarus 78, 337-354.